Journal of Nuclear Materials 458 (2015) 216–223

Contents lists available at ScienceDirect

Journal of Nuclear Materials

journal homepage: www.elsevier.com/locate/jnucmat

Helium bubble formation in ultrafine and nanocrystalline tungsten under different extreme conditions

O. El-Atwani [a,b,c,d,*], K. Hattar [e], J.A. Hinks [f], G. Greaves [f], S.S. Harilal [a,d,g], A. Hassanein [a,d]

[a] School of Nuclear Engineering, Purdue University, West Lafayette, IN 47907, United States
[b] School of Materials Engineering, Purdue University, West Lafayette, IN 47907, United States
[c] Birck Nanotechnology Center, West Lafayette, IN 47907, United States
[d] Center of Materials Under Extreme Environment, West Lafayette, IN 47907, United States
[e] Department of Radiation Solid Interactions, Sandia National Laboratories, Albuquerque, NM 87185, United States
[f] School of Computing and Engineering, University of Huddersfield, HD1 3DH, United Kingdom
[g] Pacific Northwest National Laboratory, P.O. Box 999, Richland, WA 99352, United States

HIGHLIGHTS

- Helium ion irradiation was performed on ultrafine grained and nanocrystalline tungsten.
- Irradiations were performed at different extreme conditions.
- Bubble formation and evolution were performed via ex-situ and in-situ TEM.
- Preferential bubble formation on grain boundaries occurred at displacement energies and high temperatures.
- Vacancy formation and migration is important for preferential bubble formation on grain boundaries.

GRAPHICAL ABSTRACT

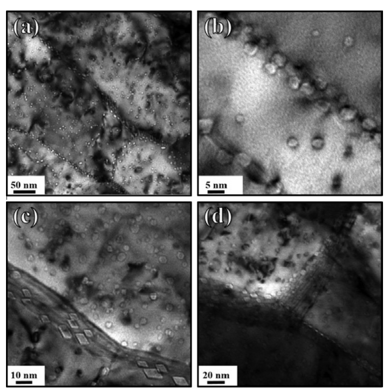

ARTICLE INFO

Article history:
Received 4 September 2014
Accepted 18 December 2014
Available online 25 December 2014

ABSTRACT

We have investigated the effects of helium ion irradiation energy and sample temperature on the performance of grain boundaries as helium sinks in ultrafine grained and nanocrystalline tungsten. Irradiations were performed at displacement and non-displacement energies and at temperatures above and below that required for vacancy migration. Microstructural investigations were performed using Transmission Electron Microscopy (TEM) combined with either in-situ or ex-situ ion irradiation. Under helium irradiation at an energy which does not cause atomic displacements in tungsten (70 eV), regardless of temperature and thus vacancy migration conditions, bubbles were uniformly distributed with no preferential bubble formation on grain boundaries. At energies that can cause displacements, bubbles were observed to be preferentially formed on the grain boundaries only at high temperatures where vacancy migration occurs. Under these conditions, the decoration of grain boundaries with large facetted bubbles occurred on nanocrystalline grains with dimensions less than 60 nm. We discuss the importance of vacancy supply and the formation and migration of radiation-induced defects on the performance of grain boundaries as helium sinks and the resulting irradiation tolerance of ultrafine grained and nanocrystalline tungsten to bubble formation.

* Corresponding author at: School of Nuclear Engineering, Purdue University, West Lafayette, IN 47907, United States.

http://dx.doi.org/10.1016/j.jnucmat.2014.12.095
0022-3115/

1. Introduction

UltraFine Grained (UFG) and NanoCrystalline (NC) metals have been proposed as radiation tolerant materials due to their high grain-boundary area [1]. The grain boundaries act as defect sinks [2,3] with large-angle grain boundaries (angles > 15°) being particularly efficient sinks [4]. Furthermore, recent work has suggested grain boundaries can facilitate Frenkel pair recombination and thus annihilation [5]. Tungsten is an important material for nuclear fusion applications due to its physical properties [6] but several irradiation studies have demonstrated considerable drawbacks due to the development of surface morphology when exposed to moderately-high helium doses [7–9]. The use of UFG and NC tungsten with high-angle grain boundaries is one of the proposed solutions to mitigate helium-induced radiation damage [10]. These materials have been shown also to possess improved mechanical properties compared to commercial coarse-grained tungsten [11,12]. In addition to being interstitial and vacancy sinks, grain boundaries in tungsten can trap helium during irradiation [13] and can thus reduce the rate of helium accumulation within the grains themselves [14]. If the observed surface morphology changes [7,8] depend on helium bubble formation as proposed in the literature [15], then engineering of grain boundary density could be a vital tool for controlling this deleterious phenomenon. It should be mentioned, however, that degradation of mechanical properties (for example, reduced creep resistance [16] or enhanced grain boundary grooving [7]) is likely to occur due to large bubble formation on the grain boundaries.

The formation of UFG and NC tungsten materials with elongated grains is achievable through several Severe Plastic Deformation (SPD) techniques [11,17]. Although their use on industrial scales remains a challenge due to limitations on the throughput achievable using current manufacturing technologies, SPD techniques can fabricate high-quality samples for important fundamental studies to gain improved understanding of physical phenomena in these materials. Whilst some theoretical studies [5,18] have demonstrated the improved radiation resistance of materials with grain boundaries, further experimental studies are crucial to validate these proposed models.

Recently, Bai et al. [5] demonstrated the effect of grain boundaries as defect sinks. It was shown that grain boundaries absorb interstitial defects and can then annihilate nearby vacancies by re-emitting the interstitial atoms back into the grain. Sefta et al. [18] used molecular dynamics to demonstrate the role of grain boundaries as helium trapping sites. In that work, the introduction of a single grain boundary was shown to result in the trapping of significantly more helium than a single crystal of tungsten.

Fundamental understanding can be acquired through studies in which the irradiation and observation of the dynamic response of a material take place simultaneously. The work reported here involved Transmission Electron Microscopy (TEM) characterization of both in-situ and ex-situ helium irradiated UFG and NC tungsten at different ion energies to control atomic displacements and different temperatures to control vacancy migration. Observation of bubble formation and evolution has given invaluable insights into the role of grain boundaries in this technologically important material.

2. Experimental

The formation of UFG and NC tungsten was performed via orthogonal machining as detailed previously [17]. The TEM samples were produced by electrochemical jet polishing with 0.5% NaOH aqueous solution at Room Temperature (RT). No significant variation in mass-thickness contrast was observed between adjacent grains in the TEM samples suggesting negligible preferential etching due to crystallographic orientation and/or grain size.

In-situ TEM during ion implantation was performed using the Microscope and Ion Accelerator for Materials Investigations (MIAMI) facility at the University of Huddersfield which is described in detail elsewhere [14] and at Sandia National Laboratories' (SNL) new in-situ ion irradiation TEM facility [19]. Ex-situ ion irradiation followed by TEM characterization were performed using the Interaction of Materials with Particles And Components Testing (IMPACT) [20] facility in the Center of Materials Under eXtreme Environments (CMUXE) at Purdue University.

Two samples were irradiated in-situ whilst under TEM observation. One sample was irradiated at SNL at RT with 8 keV helium with an angle of 15° between the ion beam and the sample surface in a JEOL JEM-2100 TEM operating at 200 kV. The other sample was irradiated at the MIAMI facility at 1223 K with 2 keV helium at an angle of 60° to the sample surface in a JEOL JEM-2000FX TEM operating at 200 kV. The ion fluxes were $\sim 3.3 \times 10^{16}$ and 1.2×10^{17} ions m^{-2} s^{-1} in the 2 keV and 8 keV experiments, respectively. The range of helium normal to the surface was calculated to be 23.6 nm (maximum ≈70 nm) and 10.6 nm (maximum ≈30 nm) for the 8 and 2 keV irradiation conditions, respectively, using the Stopping Range of Ions in Matter (SRIM) [21] Monte Carlo computer code. Two further samples were irradiated ex-situ at the IMPACT facility with 70 eV helium ions at RT and at 1173 K both at normal incidence. The ion flux in the 70 eV experiments was $\sim 1 \times 10^{19}$ ions m^{-2} s^{-1}. The range in the 70 eV experiments was calculated to be 1.4 nm (maximum ≈4 nm) using SRIM. Irradiation conditions are summarized in Table 1. Post-irradiation, samples were examined using an FEI Titan 80/300 field emission TEM and/or a JEOL JEM-3010 LaB_6 TEM both operated at 300 kV. Electron BackScattered Diffraction (EBSD) was performed on non-irradiated electrochemically polished samples using an FEI XL40 field emission scanning electron microscope equipped with an EBSD detector.

A bright-field TEM image with the associated Select Area Diffraction (SAD) pattern inserted and an EBSD orientation map of a typical UFG and NC tungsten sample used in this study is shown in Fig. 1. Ultrafine grains are defined as those having the shortest distance between opposite grain boundaries < 500 nm[12] and nanocrystalline grains as having the shortest distance <100 nm[11]. As shown in Fig. 1, both ultrafine and nanocrystalline grains coexist in the material. EBSD performed on several samples showed 40–50% of the grains to be high-angle type with grain boundary angles >15°.

Atomic displacements occur in a material if an energetic particle transfers enough energy to an atom to overcome the displacement threshold energy, E_d. The displacement energy for tungsten is reported to be 40 eV [22]. Assuming a perfectly elastic binary collision, the minimum energy a helium atom, E_{min}, requires to displace a tungsten atom can be calculated by:

$$E_{\min} = \frac{(M_{\mathrm{He}} + M_{\mathrm{W}})^2}{4M_{\mathrm{He}}M_{\mathrm{W}}} \cdot E_d \tag{1}$$

Table 1
Irradiation conditions used in the four experimental regimes (see Fig. 2) compared in this study.

Regime (see Fig. 2)	Sample temperature (K)	Helium ion irradiation		
		Energy (eV)	Flux (ions m^{-2} s^{-1})	Fluence (ions m^{-2})
I	298	70	1×10^{19}	2.5×10^{21}
II	1173	70	1×10^{19}	4.5×10^{21}
III	298	8000	1.2×10^{17}	1.5×10^{22}
IV	1223	2000	3.3×10^{16}	3.6×10^{19}